UNIVERSITY OF SOUTHAMPTON

INSTITUTE OF SOUND AND VIBRATION RESEARCH

FLUID DYNAMICS & ACOUSTICS GROUP

Active and Passive Acoustic Bubble Sizing

by

A.D. Phelps, T.G. Leighton, M.F. Schneider and P.R. White

ISVR Technical Report No. 237

October 1994

Approved: Group Chairman, Prof. P. A. Nelson

ACKNOWLEDGEMENTS

This work was funded by the Natural Environment Research Council, under SIDAL contract ref 00670.

CONTENTS

LIST OF FIGURES

ABSTRACT

This report presents the results from the research associated with a two year NERC contract funded under the SIDAL scheme. The aim of the project was to investigate methods of sizing bubbles at the moment of entrainment by passive detection of the corresponding acoustic emission, and again to actively size the existing population at a later time. The technique for measuring this so-called 'old-age' population involves sizing bubbles by means of the two frequency insonation method, and the success of examining the subharmonic sum-and-difference coupling is reported. In addition, results are presented from investigations into the variation of the subharmonic response with differing excitation amplitude and step size between successive interrogating signals, and examinations into the reproducibility of the response. Work has also been done on the passive sizing of bubbles upon entrainment with the Gabor transform technique, which gives a fast and accurate representation of the bubble's resonant frequency, of the time at which entrainment occurs, and of the amplitude of the signal.

I. INTRODUCTION

The ability to measure and count bubbles has many practical applications, including studies into decompression sickness[1] and minimising the thermal loading on power plant coolant systems[2]. Of interest to this research are investigations into how the presence of bubbles can introduce an important asymmetry into the flux of atmospheric gases into the oceans. The oceans provide a very large reservoir into which atmospheric gases dissolve[3], and bubble mediated gas exchange can result in a 1-2% supersaturation of the lower solubility gases[4,5]. When a wave breaks at sea the air trapped in a wave crest or under a plunging breaker is entrained into the ocean as a cloud of bubbles, which are then dispersed through buoyancy, dissolution, turbulence and circulatory forces, and form an 'old age' background population[6]. Information on bubble dispersal and the associated gas flux can be obtained through comparison of the air entrained in the original wave breaking process and that contained in the 'old age' population.

Acoustic techniques are very suitable for bubble sizing[7], as there is a large impedance mismatch at the gas-liquid interface. The pulsation of a bubble approximates to a lightly damped single degree of freedom system, and as such it has a well-defined resonance. For air bubbles in water at atmospheric pressure, the radius of the bubble (R_o) and the resonant frequency (υ_r) can be approximately related by:

$$\upsilon_r R_o \approx 3 \quad Hz\ m \tag{1}$$

Thus, from a knowledge of the bubble resonance, its size can readily be determined.

Passive bubble sizing techniques make use of the sound emitted from a bubble when mechanically excited, for example upon entrainment, as this 'ringing' occurs at its resonance frequency. Thus these emissions from a bubble cloud under a breaking wave or waterfall can be used to size and count the population entrained[8]. The work on passive sizing related to this project involves examining the acoustic nature of these signals, and developing a fast, accurate and automated method of interpreting these signals.

The active sizing technique employed here exploits nonlinearities in the pulsation of the bubbles, which manifest themselves at the large oscillation amplitudes associated with resonant behaviour. If the bubble is insonated with two frequencies, one a high fixed frequency ω_i (the *imaging* frequency, set at just over 1 MHz), and another lower frequency ω_p tuned to the resonant frequency of the bubble (the *pump* frequency), this nonlinear response will give rise to frequencies at $\omega_i+\omega_p$ and $\omega_i-\omega_p$[9]. Recent work[10] has shown that a *subharmonic* signal at $\omega_p/2$ can also be stimulated at resonance, and will similarly undergo sum-and-difference coupling with the imaging frequency to give emissions at $\omega_i\pm\omega_p/2$. These have been shown to be much more accurate and less ambiguous indicators of the bubble resonance frequency[11].

The results from the experimental tests are summarised later on in this document. As this is intended only as an summary of the work, many of the experimental details are omitted and results justifying some of the conclusions are left out. These details can be found in recent papers[12-16] and are referenced where appropriate.

The aims and methodology of the project, as proposed to the NERC, are 'to develop bubble sizing technology capable of characterising bubble populations both upon entrainment and in ambience. The two-year project will enable proof of concept and development, to enable, but not actually undertake, construction of an in situ device. A system to characterise the bubble population on entrainment will be constructed. An active detector will also be developed to characterise the ambient population. Having completed proof of concept using frequency analysis of the complete signal, heterodyning techniques will be introduced to enable the rapid signal processing that would be required in a field device.'

The progress made using active techniques is considerable. The nonlinear frequency coupling method has been successfully applied, and has been shown to be an extremely accurate indicator of the bubble resonant frequency. The research has involved an investigation into the parameters employed when using such a system, namely the necessary amplitude of excitation for the subharmonic response, the appropriate frequency increment between two successive projector outputs, and an examination into the reproducibility of the signal. The heterodyning system has been successfully implemented into the measurement procedure, greatly speeding up the measurement rate, and the active sizing of moving bubbles has been performed.

In addition, considerable progress has also been made into the passive sizing of bubbles upon entrainment. The work has used a specialist windowing function called the Gabor transform[17] to examine the time history of entrainment noise. This window returns a three dimensional function which gives details on the bubble resonant frequency, the time of entrainment and the amplitude of the response. This has been used to examine laboratory data, and has also been used to size the bubbles at the bottom of a small waterfall. Although the initial brief was to stop short of actual oceanic measurements and data collection, sea trials using this method were successfully performed using a four-hydrophone array deployed from a research vessel in The Solent, in the English Channel near the Isle of Wight. Details from this trial are presented in reference [16].

II. METHODS AND TECHNIQUES

Passive Tests:
The laboratory experiments were performed in a 6' x 4' x 4' glass reinforced plastic tank, which is vibration isolated by four 1400 mm x 300 mm Tico pads. Results are presented here for the entrainment of bubbles from when a continuous liquid jet impacts a water surface. The resulting acoustic emissions are detected using a Bruel and Kjaer 8104 underwater hydrophone connected to a Bruel and Kjaer type 2635 pre-amplifier. The signals are recorded onto a portable Aiwa DAT recorder, and later analysed via a MATLAB data acquisition toolbox. Data taken in the ocean during light rainfall was similarly analysed and these results are also presented.

Active Tests:
The active bubble sizing tests were also performed in the tank described above. It is a requirement for real in-situ data collection that the active collection process be automated, and so all the experiments presented here were remotely controlled from the PC and pumping frequency / data acquisition hardware. The basic bubble

insonation / data acquisition process is achieved by reading a pumping frequency value from a PC file, converting it into a sine wave and outputting it to the low frequency transducer. This tone interacts with the bubble and the imaging signal, and the resultant high frequency scattered sound field is then picked up by the high frequency receiver, processed and sampled by the acquisition hardware, and is stored onto the PC. When the data is in the memory, the next pumping frequency value is read from the output file, and so on. At the end of the whole run the data is FFTed, signal processed and displayed. This allows the bubble's dependence on two important parameters to be investigated, namely the pumping signal amplitude and the frequency step size between successive projector outputs.

These tests can be broken up into three groups. The first series of tests measured a bubble held vertically on a wire in the focus of the interrogating transducers, and employed a specialist designed data acquisition hardware package commissioned from Loughborough Sound Images[12]. This samples the scattered sound from the bubble at around 3.5 MHz, and can therefore present a complete frequency spectrum of the response of the bubble. These initial tests were important in order to fully investigate the sum-and-difference coupling phenomenon, and to ensure that the later improved signal processing techniques introduced no ambiguity or corruption of the data. The drawback of this technique is that because of the high frequency resolution required, the system has to save large amounts of data, and is thus comparatively slow (around 6 seconds per input frequency). The equipment is shown in ***figure 1***, and the relative alignment of the transducers is shown in ***figure 2***.

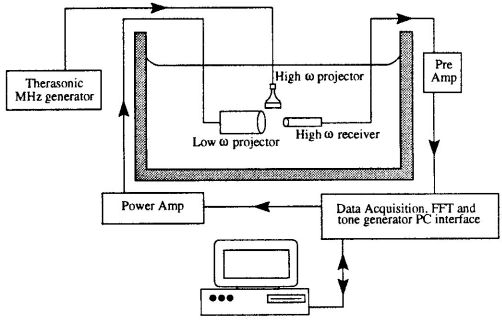

***Figure 1**: The equipment and the experimental arrangement used in the first set of active tests.*

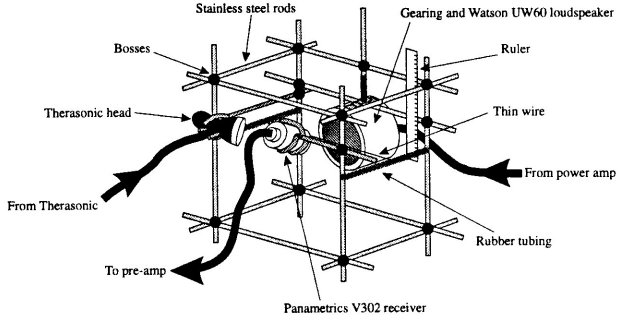

***Figure 2**: Arrangement of the active sizing transducers in a rigid cage*

The second series of tests were similarly performed on a bubble held to a wire, but instead used a hardware heterodyner to condition the returned signal from the high frequency receiver[13-15].This is employed to shift the imaging signal frequency down to D.C. and to reproduce the information contained just above the imaging signal frequency at a much lower frequency. This enables a much lower sample rate to be employed, and greatly speeds up the acquisition and processing (around 0.4 seconds per input frequency). The data acquisition and pumping tone generation is performed by a Matlab P.C. interface. The equipment schematic is shown as ***figure 3***.

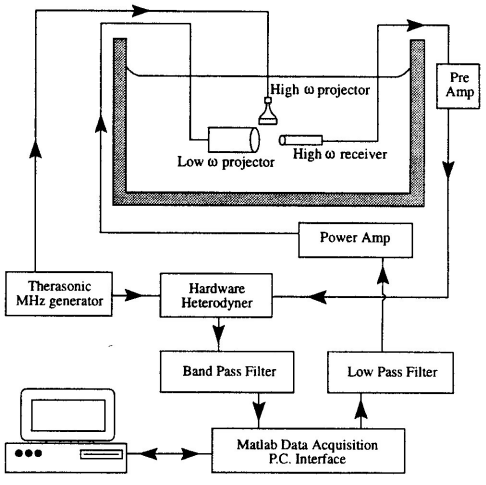

***Figure 3**: The equipment and the experimental arrangement used in the second and third set of active tests.*

With all the above tests a single bubble was employed to characterise the system, since it was important to ensure that this sizing technique, unlike others currently in operation, is not capable of erroneous triggering. However, in the third series of tests, moving bubbles were generated by compressed air from a needle below the focus of the transducers, and these were measured. These tests were performed as a direct comparison with the tests made of the bubble on the wire.

III. RESULTS

Passive Tests:

The passive sizing of bubbles upon entrainment in the laboratory is demonstrated in ***figure 4.*** This shows the time history from a jet of water directed into the tank as measured by the hydrophone. The jet was released at 25 mm above the water surface at an angle of 70° to the horizontal from a pipe of inside diameter 5 mm, and with a flow rate of 4.5 litres/min. The characteristic decaying sinusoidal responses of bubbles being entrained are evident. The Gabor transform of this data is enclosed as ***figure 5***. Each peak corresponds to the entrainment of a bubble, and its location in the mesh indicates its resonant frequency and the time at which it was formed. The passive sizing technique has been used to size and count bubbles under a waterfall

and at sea due to rain falling[16]. Size spectra of bubbles entrained in a calm sea under light rainfall are shown in ***figure 6***.

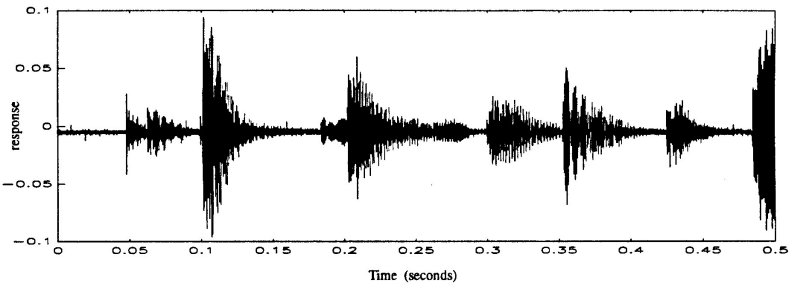

Figure 4: *Plot showing the passive bubble noise upon entrainment from a water jet. The jet was formed through a 5 mm nozzle passing 3 litres/minute at an angle of 50° to the horizontal.*

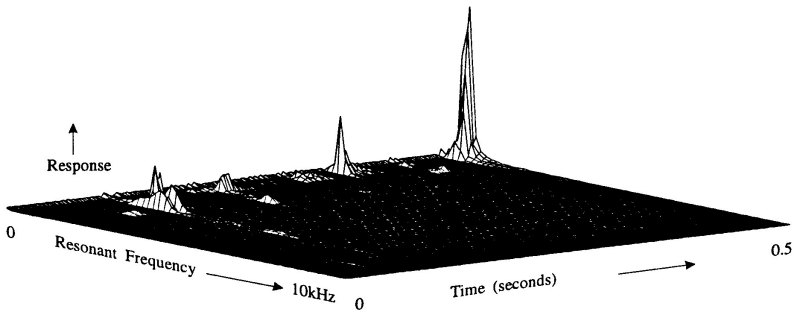

Figure 5: *Gabor transform of the water jet data from figure 4 showing time at which entrainment occurs, bubble resonance frequency and amplitude of response. Each peak corresponds to the entrainment of a single bubble.*

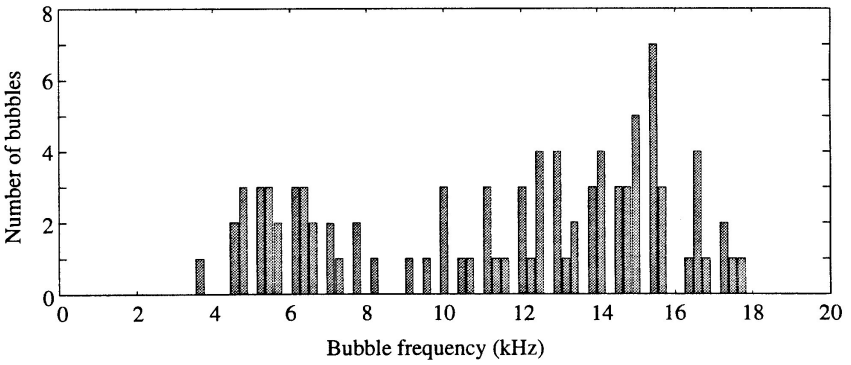

Figure 6: *Histogram of the resonance frequencies of individual bubbles measured under light rainfall at sea. The exact location of the measurements was 50° 59.962' N 1° 35.748' W.*

Active Tests:

The first series of experiments using the Loughborough Sound Images data acquisition equipment succeeded in showing that the appearance of a subharmonic signal is a far better indicator of the resonance frequency of a bubble than by examination of the $\omega_i \pm \omega_p$ response. This is demonstrated in ***figure 7***, with the full

results presented in reference[12]. The plot shows the data acquisition unit output over twenty different pumping frequencies, going from 1925 Hz to 2400 Hz in 25 Hz steps. The main ridge which is constant over the twenty tests is the imaging signal from the Therasonic frequency generator, with spurious side lobes either side of its centre peak. In front of this is a second broken ridge which similarly is present over all twenty pumping signals - this is the coupled response corresponding to $\omega_i+\omega_p$. Between the two bands is a single peak which occurs at a pumping frequency of 2275 Hz. This is due to the subharmonic emission from the bubble, and is located at $\omega_i+\omega_p/2$. The peak returned from the subharmonic is not only considerably narrower than that of the fundamental, but stands far higher above the noise floor than the $\omega_i+\omega_p$ signal. Further work has shown that the $\omega_i\pm\omega_p$ signal can arise from the direct coupling of the two interrogating sound fields in the absence of a bubble, although this is 10-15 dB below the level caused by the nonlinear mixing action of a bubble. Therefore bubble sizing solely using the signal at $\omega_i\pm\omega_p$ would not provide an unambiguous indicator of the presence of a bubble.

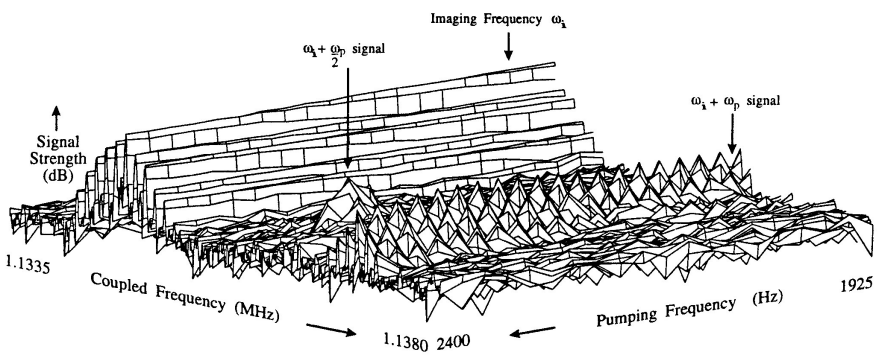

***Figure 7**: Mesh plot of returned signal strength through a bubble's resonance for the single tethered bubble tests with no hardware heterodyning.*

Tests were also performed to investigate the dependence of the output response on the level of the pumping signal. Using the same bubble throughout, the height of the subharmonic signal was measured over a series of runs through its resonance location in 5 Hz steps, with the amplitude of the pumping frequency signal raised slightly each time. These experiments show that a definite excitation threshold exists, below which no signal is present and above which a peak appears in the signal with an unambiguous maximum - this can be used to very accurately determine the resonant frequency of the bubble. However, when the bubble is insonated above this threshold the response becomes overdriven, and there is an increase in the frequency range of the pumping signal over which a subharmonic can be exacted. Therefore the exact location of the bubble's resonant frequency becomes less obvious. Such results indicate that the choice of pumping amplitude is critical for bubble sizing. These tests showed the amplitude location of this threshold to be around 70 Pa (0-pk) for a 2500 Hz resonant bubble.

The reproducibility of the subharmonic signals were also tested by repeating an identical run five times, and looking for the maximum value of the fundamental and subharmonic sum-and-difference responses. Data was collected when the bubble was insonated at its subharmonic threshold, and again when overdriven. The results show

a considerably larger amplitude spread for the subharmonic signal than for the fundamental sum-and-difference signal. This may mean that it is more favourable to use the subharmonic signal to locate the bubbles, and the height of the fundamental signal to count the number occurring in that frequency band.

The second series of tests used a hardware heterodyner to shift the bubble response to above D.C., and thus speed up the processing. A result of this technique is shown in ***figure 8***, and the full results are presented in the papers reference [13-15]. Here the bubble is insonated between 1700 and 2700 Hz in 25 Hz steps, and the plot shows the frequency response from 0 to 3400 Hz. As a result of the heterodyning process, the signal contained above the imaging frequency is overlaid with that below it, so that every peak is a sum of the $\omega_i+\omega_p$ and the $\omega_i-\omega_p$ signals. Similarly to the series one mesh plot, the figure shows the $\omega_i\pm\omega_p$ ridge present over the entire 41 pumping tones, and a considerably clearer subharmonic peak at $\omega_i\pm\omega_p/2$.

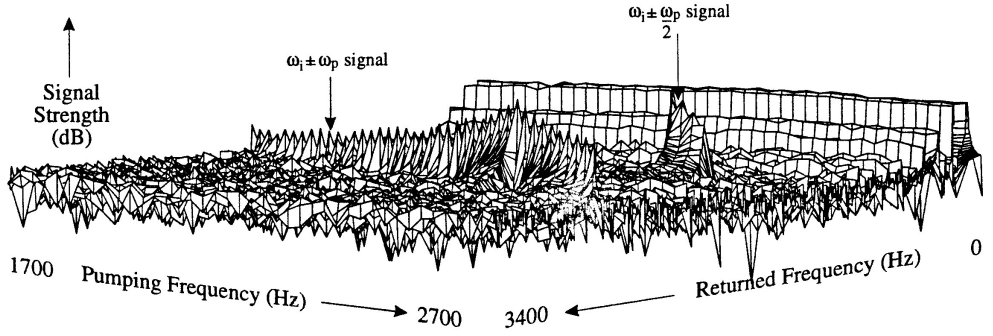

***Figure 8**: Mesh plot of returned signal strength through a bubble's resonance for the single tethered bubble tests employing hardware heterodyning.*

Because of the greatly improved sampling and processing time, it was possible to repeat the experiments to determine the subharmonic threshold for a large number of bubbles. Thirty bubbles were examined and the location of their amplitude threshold was noted by stepping through their resonance in 5 Hz increments. This was determined to be around 35 Pa for bubbles resonant between 2000 Hz and 3200 Hz. The reason for this apparent discrepancy with the threshold measurements performed in the first series of tests is probably due to surface tension effects - the cleanness of the water, the area of contact with the wire, etc. can all influence this, and therefore only order of magnitude measurements are appropriate[18].

Using the data collected during the threshold measurements, the frequency span of the subharmonic signal was also measured for each increasing pumping signal amplitude, and the amplitudes at which these frequency spans passed 25 Hz, 50 Hz and 100 Hz were noted. This showed two things - firstly that the 25 Hz span fell almost exactly on the threshold line, indicating that there is a minimum practical step size to interrogate the bubble population with even with a careful choice of pumping signal amplitude, and secondly that as the pumping amplitude was turned up and the frequency span increased, the width of the subharmonic signal became harder to predict. This suggests that there is also a maximum practical step size past which it

becomes unclear whether one is measuring every bubble or measuring the same one twice.

The third series of experiments was concerned with moving bubbles which were released through a needle underneath the cage such that they rose through the focus of the transducers one at a time. By ensuring that a large pressure drop occurs at the tip of the needle, the bubbles can be created all the same size[18]. The results of a sweep through their resonance location is shown in ***figure 9*** as a grey-scale map: the signal content is unclear when shown on a mesh plot as the returned signal has a variable strength due to the changing position of a bubble in the transducer focus from one pump output to the next, and a Doppler shift on the data peaks. The data in ***figure 9*** was swept between 3500 Hz and 4500 Hz in 25 Hz steps, and it shows the double peaked ridge of the $\omega_1 \pm \omega_p$ signal (after the Doppler shift and the heterodyning both the $\omega_1+\omega_p$ peak and the $\omega_1-\omega_p$ peak are evident) and a clear subharmonic at ~4300 Hz.

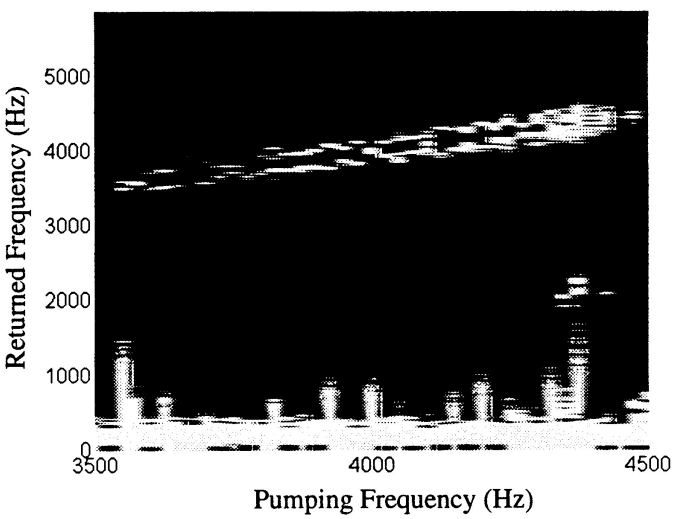

***Figure 9**: Grey-scale map of returned signal strength through a bubble's resonance for the train of rising bubble tests employing hardware heterodyning.*

Tests have also been performed on these free rising bubbles to determine the location of the subharmonic threshold, which for 3000 Hz resonant bubbles appears to be located at around 140 Pa, which is slightly higher than was measured for bubbles on a wire. By means of verifying these results, numerical models describing the dynamics of acoustically excited bubbles were investigated. Three different models were implemented, namely (in order of increasing sophistication) the Rayleigh-Plessett equation, the Keller equation and the Gilmore equation[7]. These were numerically realised by computer on an assumed 1 mm radius bubble driven at its linear resonance using a fifth order Runge-Kutta solution. The results suggest that a subharmonic will form either when the bubble is driven at twice its resonant frequency at approximately 20,000 Pa, or that it can be exacted from a resonant bubble at around 150,000 Pa. These amplitudes are orders of magnitude higher than the experimentally achieved thresholds, suggesting that a mechanism other than volumetric pulsations may be responsible for the subharmonics. Earlier work has shown the presence of surface ripples around the bubble at resonance[10], and these have been shown to be

excited at half the driving frequency[20]. The threshold for surface stability above which these waves occur can be calculated, and has been shown to be of the same order as the experimental thresholds[20].

IV. CONCLUSIONS

Continuing the studies reported in reference [21], the work has demonstrated the potential for sizing bubbles both passively and actively. The specialist Gabor transform has been successfully employed to passively detect the bubbles' characteristic transient signal upon entrainment, and has been used to size bubbles both in the laboratory and during actual sea trials. The active tests, which uses a technique which examines the nonlinear coupling of two incident sound fields on the bubble, gives evidence that locating the resonant frequency by looking for the subharmonic emission at $\omega_i \pm \omega_p/2$ is a more accurate and unambiguous indicator than by looking for a signal at $\omega_i \pm \omega_p$. This subharmonic signal appears to only exist above a well defined insonation amplitude level threshold, but for only small increases in amplitude above this threshold the range of pumping frequencies over which a signal can be exacted increases rapidly. Tests performed on single size bubbles both tethered to a wire and free-rising through the common focus of the transducers have demonstrated that this subharmonic threshold is considerably lower than that predicted using mathematical models for the volumetric pulsation of bubbles: this suggests that another mechanism is responsible for the appearance of the subharmonic signal, most probably surface waves generated over the surface of the bubble.

V. REFERENCES

1. **Kisman, K.** Spectral analysis of Doppler ultrasonic decompression data *Ultrasonics* (1977) **15** 105-110

2. **Hulshof, H.J.M. and Schurink, F.** Continuous ultrasonic waves to detect steam bubbles in water under high pressure *Kema Scientific & Technical Reports* (1985) **3** 61-69

3. **Anderson, I. and Bowler, S.** Oceans spring surprise on climate modellers *New Scientist* (1990) **125** 24

4. **Woolf, D.K.** Bubbles and the air-sea transfer velocity of gases *Atmosphere-Ocean* (1993) **31** 451-474

5. **Woolf, D.K. and Thorpe, S.A.** Bubbles and the air-sea exchange of gases in near-saturation conditions *J. Marine Res.* (1991) **49** 435-466

6. **Monahan, E.C. and Lu, N.Q.** Acoustically relevant bubble assemblages and their dependence on meteorological parameters *IEEE J. Oceanic Eng.* (1990) **15** 340-349

7. **Leighton, T.G.** The Acoustic Bubble (1994) *Pub. Academic Press, UK*

8. **Leighton, T.G. and Walton, A.J.** An experimental study of the sound emitted from gas bubbles in a liquid *Eur. J. Phys.* (1987) **8** 98-104

9. **Newhouse, V.L. and Shankar, P.M.** Bubble size measurement using the nonlinear mixing of two frequencies *JASA* (1984) **75** 1473-1477

10. **Leighton, T.G., Lingard, R.J., Walton, A.J. and Field, J.E.** Acoustic bubble sizing by combination of subharmonic emissions with imaging frequency *Ultrasonics* (1991) **29** 319-323

11. **Hardwick, A.J., Leighton, T.G., Walton, A.J. and Field, J.E.** Acoustic bubble sizing through nonlinear combinations involving parametric excitations *European Conf. on Underwater Acoustics* (Ed. M. Weydert) pub. Elsevier Applied Science (1992) 153-156

12. **Phelps, A.D. and Leighton, T.G.** Investigations into the use of two frequency excitation to accurately determine bubble sizes *IUTAM Symposium on Bubble Dynamics and Interface Phenomena, Birmingham, UK* (Ed J. Blake) pub. Kluwer Academic Press (1993) 475-484

13. **Phelps, A.D. and Leighton, T.G.** Automated bubble sizing using two frequency excitation techniques *3rd Conf. on Sea Surface Sound, California USA - Ed M. Buckingham* (in press) (1994)

14. **Phelps, A.D. and Leighton, T.G.** Acoustic bubble sizing using two frequency excitation techniques *2nd Conf. on Underwater Acoustics, Copenhagen, Denmark* (Ed. L. Bjørnø) pub. European Commission (1994) 201-206

15. **Phelps, A.D. and Leighton, T.G.** High resolution bubble sizing through detection of the subharmonic response with a two frequency excitation technique. *J. Acoust. Soc. Am.* Submitted.

16. **Leighton, T.G., Schneider, M.F. and White, P.R.** Study of bubble fragmentation using optical and acoustic techniques. *3rd Conf. on Sea Surface Sound, California USA - Ed M. Buckingham* (in press) (1994)

17. **Friedlander, B. and Porat, B.** Detection of transient signals by the Gabor representation *IEEE Trans. Acoust, Speech, Signal Processing* (1989) **37** 169-180

18. **Exner, M.L. and Hampe, W.** Experimental determination of the damping of pulsating air bubbles in water *Acustica* (1953) **3** 67-72

19. **Clift, R., Grace, J.R. and Weber, M.E.** Bubbles, drops and particles (1978) *Pub. Academic Press, New York, USA*

20. **Neppiras, E.A.** Acoustic cavitation *Physics Reports* (1980) **61** 161-251

21. **Phelps, A.D., Leighton, T.G., Schneider, M.F. and White, P.R.** Acoustic bubble sizing, using active and passive techniques to compare ambient and entrained populations *ISVR Technical Report No. 229* (1994)